Published in final edited form as:
*J Biol Chem*. 2007 September 28; 282(39): 28431–28440. doi:10.1074/jbc.M706176200.

# PLASMA MEMBRANE TARGETING IS ESSENTIAL FOR REM-MEDIATED CA$^{2+}$ CHANNEL INHIBITION‡

**Robert N. Correll**[*], **Chunyan Pang**[*], **Brian S. Finlin**[*], **Alexandria M. Dailey**[*], **Jonathan Satin**[#,1], and **Douglas A. Andres**[*]

[*] Department of Molecular and Cellular Biochemistry, University of Kentucky College of Medicine, Lexington, Kentucky 40536-0509

[#] Department of Physiology, University of Kentucky College of Medicine, Lexington, Kentucky 40536-0509

## Abstract

The small GTPase Rem is a potent negative regulator of high voltage-activated $Ca^{2+}$ channels and a known interacting partner for $Ca^{2+}$ channel accessory β subunits. The mechanism for Rem-mediated channel inhibition remains controversial, though it has been proposed that $Ca_V\beta$ association is required. Previous work has shown that a C-terminal truncation of Rem ($Rem^{1-265}$) displays reduced *in vivo* binding to membrane-localized β2a and lacks channel regulatory function. In this paper we describe a role for the Rem C-terminus in plasma membrane localization through association with phosphatidylinositol lipids. Moreover, $Rem^{1-265}$ can associate with β2a *in vitro*, and β1b *in vivo*, suggesting that the C-terminus does not directly participate in $Ca_V\beta$ association. Despite demonstrated β1b binding, $Rem^{1-265}$ was not capable of regulating a $Ca_V1.2$/β1b channel complex, indicating that β subunit binding is not sufficient for channel regulation. However, fusion of the CAAX domain from K-Ras4B or H-Ras to the $Rem^{1-265}$ C-terminus restored membrane localization and $Ca^{2+}$ channel regulation, suggesting that β binding and membrane localization are independent events required for channel inhibition.

## Introduction

High voltage-activated $Ca^{2+}$ channels ($Ca_V1$ and $Ca_V2$ families) transduce electrical activity into increased intracellular calcium that mediates a diverse array of essential cellular processes including hormone secretion, neurotransmitter release, and excitation-contraction coupling in muscle systems (1). The cardiac L-type $Ca^{2+}$ channel is a multiprotein complex consisting of the pore-forming $Ca_V1.2$ α-subunit and auxiliary subunits including $Ca_V\beta$ and $\alpha_2$-δ subunits (1). The $Ca_V\alpha$ subunit determines the ion selectivity and single channel conductance of the mature channel while co-expression of $Ca_V\beta$ or $\alpha_2\delta$ facilitates cell surface trafficking of the $\alpha_1$-subunit, increases $Ca^{2+}$ current amplitude, and alters channel gating properties (1,2). $Ca_V\beta$ subunits are encoded by four genes (β1-β4), each subject to complex splicing (3). $Ca_V\beta2a$, a β isoform found in the heart, is subject to postranslational

‡This work was supported by Public Health Service Grants HL072936 (to D. A. A.), HL074091 (to J. S.), and P20 RR20171 from the National Center for Research Resources, National Institutes of Health (to D. A. A.), an American Diabetes Association Junior Faculty award (to B. S. F.), and an American Heart Association pre-doctoral fellowship and an NIH Interdisciplinary Cardiovascular Training Grant T32 HL072743 (to R. N. C.).

Address correspondence to: Douglas A. Andres, Dept. of Molecular and Cellular Biochemistry, BBSRB Rm. B-179, University of Kentucky College of Medicine, 741 South Limestone St., Lexington, KY 40536-0509. Tel.: 859-257-6775; Fax: 859-323-1037; dandres@uky.edu.
[1]An Established Investigator of the American Heart Association.

palmitoylation which directs plasma membrane localization, while other β isoforms are predominantly localized to the cytosol when not bound to $Ca_V\alpha_1$ (3).

Recently, members of the RGK family of Ras-related GTPases, including Rem (4), Rem2 (5), Rad (6), and Gem/Kir (7), have been identified as potent regulators of HVA $Ca^{2+}$ channel function (8–10). Although all RGK GTPases associate with $Ca_V\beta$ subunits and prevent *de novo* expression of L-type $I_{Ca}$ (8–10), the mechanism of RGK protein-mediated $Ca^{2+}$ channel inhibition remains controversial. It was originally hypothesized that RGK protein binding blocked $Ca_V\alpha1/\beta$ association leading to a reduction of functional channels at the cell surface (8,11–14). However, a series of recent studies suggest instead that the majority of RGK proteins inhibit the activity of the preassembled channel complex at the plasma membrane (10,15,16), although $Ca_V\beta$ association still appears critical (16,17). Moreover, RGK-mediated channel regulation appears more complex than simple $Ca_V\beta$ sequestration (16,17), and may include contributions from both the $Ca_V\alpha_1$ C-terminus and PKA signaling pathways (18).

The conserved RGK C-terminus plays a crucial role in $Ca^{2+}$ channel regulation. Deletion of the Rem, Rem2, and Rad C-terminus inhibits plasma membrane localization of the proteins, greatly reduces $Ca_V\beta2a$ subunit binding, and eliminates $Ca^{2+}$ channel regulation (9,15,19). Recent work has described mutations to the C-terminal domain that alter CaM and 14-3-3 binding in all RGK proteins (12–14,20), and research by Beguin and colleagues suggests that loss of CaM binding leads to nuclear localization, while overexpression of 14-3-3 proteins promotes the clearance of RGK proteins from the nucleus (12–14). Mutations that prevent 14-3-3 and CaM binding in Rad result in the redistribution of Rad and $Ca_V\beta3$ to the nucleus (14). A corresponding loss of Rad-mediated $Ca^{2+}$ channel regulation for these mutants has led to the suggestion that RGK-mediated channel inhibition involves nuclear targeting of $Ca_V\beta$-subunits (14). Thus, while it is clear that the conserved RGK C-terminus plays a role in channel regulation, the exact mechanism of action remains to be determined.

Here, we analyze the contribution of the Rem C-terminus to $Ca^{2+}$ channel regulation. We find that Rem is trafficked to the plasma membrane, associates with phosphatidylinositol lipids, and that truncation of the C-terminus results in redistribution to the cytosol, accompanied by a loss of calmodulin binding and $Ca^{2+}$ channel inhibition. These truncation mutants display a reduction in $Ca_V\beta2a$, but not $Ca_V\beta1b$ association *in vivo*, and loss of the C-terminus does not affect *in vitro* β2a subunit binding, indicating that β subunit interaction does not require the Rem C-terminus. In addition, the $Rem^{1\text{-}265}$ truncation mutant which binds $Ca_V\beta1b$ does not inhibit current expression from the heterologously expressed $Ca_V1.2/Ca_V\beta1b$ channel, indicating that Rem does not inhibit channel function solely through β subunit sequestration. Anchoring of $Rem^{1\text{-}265}$ to the plasma membrane using the CAAX motif from H-Ras or K-Ras4B restores $Ca^{2+}$ channel inhibition, suggesting that plasma membrane localization is critical for Rem-mediated $Ca^{2+}$ channel regulation.

## Experimental Procedures

### Plasmids

Mammalian expression vectors for $Ca_V1.2$ α-subunit, FLAG epitope-tagged β2a subunit, FLAG epitope-tagged β1b subunit, and HA epitope-tagged Rem have been described previously (9). Rem truncation mutants were generated by PCR using HA-tagged Rem as the template and fully sequenced. RFP-$Rem^{266\text{-}297}$ was generated by PCR and inserted behind RFP in pDsRed vector (Clontech). Chimeric Rem proteins were generated by ligation of oligonucleotides corresponding to the C-terminus of human K-Ras4B (171-188) or mouse H-Ras (171-189) to the C-terminus of pcDNA3.1+zeo 3xHA-$Rem^{1\text{-}265}$ utilizing XbaI/ApaI sites.

## Confocal Imaging

Confocal imaging of GFP-tagged Rem truncations, chimeric Rem proteins, RFP-$Rem^{266-297}$ and $Rem^{WT}$ was performed as previously described (18). Images displayed are representative of the cells observed. Quantification was performed using Leica LCS software. Plasma membrane localization was quantified by four line-scan intensity measurements through each cell beginning in the central cytoplasm, avoiding the nucleus, and ending at the cell periphery. GFP intensity at the cell periphery in each scan was divided by the mean intensity over the entirety of the scanned line to monitor GFP cell periphery intensity over that of the GFP-tagged protein in the cytosol. Line-scans were averaged for each cell, and the mean values of the averaged cell measurements are reported as mean ± SE. Significance was determined using Student's t-test with p-value of <0.05. To examine the localization of GFP-$Rem^{1-276}$ at the cell periphery, a double-blind study was performed. From the line-scan analysis above, 32 cells expressing $Rem^{1-276}$ and 33 cells expressing $Rem^{1-265}$ were randomized and examined by three individuals, who were asked to score each cell for the presence of increased punctate GFP fluorescence at the cell periphery. Scored cells were then matched to their appropriate treatment and the percentage of cells from each treatment displaying localized increases of GFP fluorescence at the cell boundary determined. Values are reported as mean ± standard deviation and significance was determined using Student's t-test with p-value of <0.05.

## PIP Binding Assay

3x Flag-tagged Rem truncations or empty 3xFlag vector were expressed in tsA201 cells using the calcium phosphate transfection method as described previously (21). 48 hours post-transfection, cells were harvested and lysed in PIP binding buffer (50 mM Tris-HCl (pH 8.0), 10 mM EDTA (pH 8.0), 100 mM NaCl, 0.5% Triton X-100, 1x protease inhibitor cocktail I (Calbiochem)), sonicated, and centrifuged at 100,000 × *g*. PIP strips (Molecular Probes) were blocked in TBS-T + 3% fatty-acid-free BSA for one hour and incubated with total cell lysate from the appropriate treatment in TBS-T + 3% fatty-acid-free BSA at 4°C overnight with gentle rocking. Membranes were then washed with TBS-T supplemented with 3% fatty-acid-free BSA and probed with biotinylated FLAG antibody and HRP-conjugated streptavidin. Binding of Rem truncations was detected using enhanced chemiluminescence reagent (Pierce).

## β-subunit Association Assays

Co-immunoprecipitation of 3xHA-tagged Rem truncations, chimeric Rem proteins, and $Rem^{WT}$ with $Ca_V\beta 2a$ and $Ca_V\beta 1b$ in HEK293 and tsA201 cells were performed as previously described (9,21).

## Calmodulin Binding

TsA201 cells were maintained in DMEM (Gibco) supplemented with 10% FBS (Gibco) and transfected with the indicated plasmids using the calcium-phosphate method as previously described (21). 48 hours post-transfection, cells were harvested and lysed in calmodulin IP buffer (50 mM Tris-HCl (pH 7.4), 150 mM NaCl, 0.5% Nonindet P-40, 1x phosphatase inhibitor cocktail II (Calbiochem), 1x protease inhibitor cocktail I (Calbiochem), 1 mM PMSF), sonicated, and centrifuged at 100,000 × *g*. Calmodulin-sepharose beads (GE Healthcare) were washed 2x with IP buffer and incubated with 1 mg of total lysate in the presence of 2 mM $CaCl_2$ or 2.5 mM EGTA. Beads were washed 3x in IP buffer containing 2 mM $CaCl_2$ or 2.5 mM EGTA as appropriate and proteins were released from the beads by boiling 5 minutes in 20 μL 2xSDS-PAGE loading buffer. Associated proteins were resolved on 10% SDS-PAGE minigels and transferred to nitrocellulose membranes. Interaction of

Rem proteins with calmodulin was examined by immunoblot with Rem polyclonal antibody (9).

### In Vitro Rem Binding Assay

Generation of GST-tagged $Rem^{1-265}$ vector, as well as protein production and purification have been previously described (4,9). Generation of *in vitro* transcribed/translated $^{35}S$-labeled $Ca_V\beta2a$, and the *in vitro* binding assay with GST-tagged Rem have been previously described (16).

### Electrophysiology

HEK293 cells were transfected using Effectene (Qiagen) according to the manufacturer's instructions. TsA201 cells were transfected with the indicated plasmids using the calcium phosphate method as previously described (21) and whole-cell patch clamp experiments were performed as described previously (21). Pipette solutions (in mM) consisted of 150 CsCl, 1 $MgCl_2$, 5 Mg-ATP, 3 EGTA, 5 Hepes (pH 7.36). The bath solution for $Ba^{2+}$ recordings (in mM) consisted of 112.5 CsCl, 30 $BaCl_2$, 1 $MgCl_2$, 10 tetraethylammonium chloride, 5 glucose, 5 Hepes (pH 7.4). The bath solution for $Ca^{2+}$ recordings (in mM) consisted of 112.5 CsCl, 30 $CaCl_2$, 1 $MgCl_2$, 10 tetraethylammonium chloride, 5 glucose, 5 Hepes (pH 7.4). Traces were analyzed using Origin statistical software. Values reported as normalized mean at 5 mV ± SE for $Ba^{2+}$ currents, and as normalized mean at 15 mV ± SE for $Ca^{2+}$ currents, and significance was determined using Student's t-test with p-value of <0.05. Voltage curves were fit to the Boltzmann form:

$$I(V)=G_{max} * (V - E_{rev})/(1+exp(V_{1/2} - V)/k)$$

Electrophysiological parameters of the analyzed currents are reported in Table 1.

## Results

### The Rem C-terminus is Required for Plasma Membrane Trafficking

Previous studies have shown that Rem has a complex subcellular distribution, as it is found in both the cytosol and in association with the plasma membrane when expressed in a variety of cells (5,18,22,23). Since Rem has been shown to directly interact with $Ca_V\beta$-subunits, and this association appears to be required for Rem-mediated blockade of surface localized $Ca^{2+}$ channels, we used confocal microscopy to examine whether $Ca_V\beta2a$ subunit expression modulates Rem trafficking to the plasma membrane. As seen in Fig. 1*B*, GFP-$Rem^{WT}$ displayed a border-enriched fluorescence pattern, consistent with localization to the plasma membrane. Fluorescence was also observed in the cytosol, but was excluded from the nucleus. The distribution of GFP-$Rem^{WT}$ co-expressed with pCMVT7/F2 (control vector) was statistically indistinguishable from GFP-$Rem^{WT}$ co-expressed with either Flag-$Ca_V\beta2a$, $Ca_V1.2$, or Flag-$Ca_V\beta2a$+$Ca_V1.2$ (Fig. 1*B*). Thus, plasma membrane localization of Rem likely involves an intrinsic membrane targeting domain and is not greatly influenced by interactions with $Ca^{2+}$ channel subunits.

To identify the structural domain in Rem responsible for plasma membrane trafficking, we generated a series of Rem C-terminal truncation mutants fused to green fluorescent protein (GFP) and examined their subcellular distribution using confocal microscopy in the presence of co-expressed empty Flag vector control, Flag-$Ca_V\beta2a$, $Ca_V1.2$, or Flag-$Ca_V\beta2a$+$Ca_V1.2$ (Fig. 1*C*). Once again, co-expression of $Ca_V$ subunits had no measurable effect on Rem mutant localization (Fig. 1*C*). Intensity profiling analysis (Fig. 1*D*) revealed that both GFP-$Rem^{1-282}$ (5.05 ± 0.36, n=40) and GFP-$Rem^{WT}$ (2.89 ± 0.30, n=28) were prominently

localized to the cell periphery in a manner consistent with plasma membrane localization, and surprisingly, that $Rem^{1-282}$ displayed significantly stronger targeting than $Rem^{WT}$ ($p < 0.001$), perhaps suggesting that the distal C-terminus plays a regulatory role in Rem localization. GFP-$Rem^{1-276}$ (1.22 ± 0.02, n=43) displayed only a slight enrichment at the cell periphery using this analysis, however this truncation did show a statistically significant increase in membrane localization when compared to $Rem^{1-270}$ (1.03 ± 0.01, n=58) or $Rem^{1-265}$ (0.99 ± 0.02, n=55) which were expressed exclusively in the cytosol ($p < 0.001$) (Fig. 1*C*, *D*). To understand this difference, we more closely examined the distribution of the GFP-Rem truncations by double-blind trial and noted that rather than a uniform membrane pattern of fluorescence, 73.96 ± 12.63% of cells expressing GFP-$Rem^{1-276}$ displayed a punctate pattern of fluorescence at the cell boundary (Fig. 1*E*), as compared to 15.15 ± 13.21% of cells expressing GFP-$Rem^{1-265}$ ($p < 0.01$). Taken together, these data suggest that residues 270-282 within the Rem C-terminus play a critical role in targeting Rem to the plasma membrane.

## Truncation of the Rem C-terminus Disrupts PI Lipid Binding

Recent data suggests that many small GTPases bearing polybasic C-termini are plasma membrane localized and bind phosphatidylinositol (PI) lipids, including the Gem and Rad GTPases (23). To examine whether the Rem C-terminus also directs selective PI lipid binding, we performed an overlay assay utilizing 3xFlag-tagged $Rem^{WT}$ and Rem C-terminal truncations, or empty 3xFlag vector control, overexpressed in tsA201 cells, and PIP strips (Molecular Probes), Hybond membranes spotted with 15 different biologically-active lipids. As shown in Fig. 2, $Rem^{WT}$ and $Rem^{1-282}$ displayed strong association with PtdIns(3)P, PtdIns(4)P, PtdIns(5)P, PtdIns(3,4)$P_2$, PtdIns(3,5)$P_2$, PtdIns(4,5)$P_2$, PtdIns(3,4,5)$P_3$, and phosphatidic acid, while greater C-terminal truncations resulted in substantially diminished lipid binding. These data correlate with the observed reduction in plasma membrane association (Fig. 1*C*, *D*), and suggest that membrane localization is mediated in part by association of the Rem C-terminus with phosphatidylinositol lipids.

## Contribution of the C-terminus to Rem-mediated $Ca^{2+}$ Channel Regulation

The Rem truncation mutant $Rem^{1-282}$ retains the ability to bind β2a and regulate $Ca^{2+}$ channel activity, while $Rem^{1-265}$ is incapable of HVA $Ca^{2+}$ channel regulation and displays reduced β2a binding (9). However, as $Rem^{1-265}$ is not plasma membrane localized (Fig. 1*C*, *D*), we next asked whether the intermediate Rem truncations were capable of binding β2a and regulating $Ca^{2+}$ channel function. To this end, 3xHA-tagged versions of $Rem^{1-265}$, $Rem^{1-270}$, $Rem^{1-276}$ and $Rem^{WT}$ were analyzed for β2a binding (Fig. 3*A*). As reported previously, $Rem^{1-265}$ displayed an almost complete loss of association with Flag-β2a (9) as measured by co-immunoprecipitation, while binding of $Rem^{1-270}$ to β2a was noticeably weaker than that between Flag-β2a and $Rem^{WT}$ or $Rem^{1-276}$.

Interestingly, while co-expression of either $Rem^{WT}$ or $Rem^{1-282}$ has been shown to result in a complete blockade of ionic current expression (9), neither $Rem^{1-270}$ or $Rem^{1-276}$ was capable of generating a complete channel block in the presence of 30 mM $Ba^{2+}$ (Fig. 3*C*, *E*). Whole-cell currents elicited in the presence of GFP-$Rem^{1-270}$ co-expression (−11.877 ± 4.128, n=9) were statistically indistinguishable from control currents in HEK293 cells expressing $Ca_V1.2$+Flag-β2a+GFP (−9.326 ± 1.914, n=7) (Fig. 3*E*) suggesting that this truncation mutant has lost the ability to regulate $Ca^{2+}$ channel activity. On the other hand, currents measured in the presence of $Rem^{1-276}$ co-expression (−1.326 ± 0.627, n=7) are 86% lower than control currents ($p < 0.01$) (Fig. 3*E*), but did not result in the complete block of current seen with $Rem^{WT}$. As $Rem^{1-276}$ displayed a slight, but statistically significant increase in cell periphery localization when compared to $Rem^{1-265}$ and $Rem^{1-270}$ (Fig. 1*D*),

it is possible that the difference in $Ca^{2+}$ channel inhibition is due to a defect in membrane localization.

Recent studies have suggested that calmodulin association is critical for both Gem and Rad-dependent $Ca^{2+}$ channel regulation (12,14,20), but the importance of calmodulin to Rem-mediated channel regulation is less clear (14). To explore this issue, we next examined the ability of the Rem truncations to regulate $Ca_V1.2/Ca_V\beta2a$ channel complexes with 30 mM $Ca^{2+}$ as charge carrier. Although GFP-$Rem^{1-276}$ was not capable of completely inhibiting current expression in this system (−1.212 ± 0.609, n=13), currents obtained for $Ca_V1.2$+Flag-β2a+GFP-$Rem^{1-276}$ were not significantly different from those seen in the presence of GFP-$Rem^{WT}$ (−0.493 ± 0.258, n=9), most likely due to the smaller currents expressed in this system (Fig. 3*D*, *F*). As seen in Fig. 3*B*, in a calmodulin-sepharose binding assay, only $Rem^{WT}$ and $Rem^{1-282}$ displayed $Ca^{2+}$-dependent calmodulin binding. Since $Rem^{1-276}$ is capable of partial channel regulation, these data suggest that calmodulin association is not required for Rem-mediated $Ca^{2+}$ channel regulation.

## $Ca_V\beta$ Association is not Sufficient for Rem-mediated $Ca^{2+}$ Channel Inhibition

We next investigated whether the C-terminus directly contributed to $Ca_V\beta2a$ association or if the effect was indirect, resulting from relocalization of Rem to the cytosol. To this end, the ability of recombinant $^{35}S$-labeled $Ca_V\beta2a$ to associate with recombinant GST-$Rem^{1-265}$ was examined. As shown in Fig. 4*A*, in the absence of a cellular context, radiolabeled $Ca_V\beta2a$ displays binding to GST-$Rem^{1-265}$. To extend this analysis, we next asked whether the Rem C-terminus was necessary for *in vivo* association with a β-subunit isoform ($Ca_V\beta1b$), which, like $Ca_V\beta2a$ is localized to the plasma membrane, but is not palmitoylated and is thought to be targeted to the cell surface through its C-terminus (3). Lysates from tsA201 cells co-expressing HA-tagged $Rem^{1-265}$ or $Rem^{WT}$ and empty vector (control) or Flag-tagged $Ca_V\beta1b$ were subjected to anti-Flag immunoprecipitation analysis, and bound HA-tagged proteins were visualized by SDS-PAGE and immunoblotting. HA-$Rem^{1-265}$ and HA-$Rem^{WT}$ proteins bind $Ca_V\beta1b$ with approximately equal efficiency (Fig. 4*B*), demonstrating that the Rem C-terminus plays no direct role in $Ca_V\beta1b$ binding *in vivo*.

To determine whether $Ca_V\beta1b$ binding was alone sufficient to regulate channel function, we next examined the ability of both $Rem^{WT}$ and $Rem^{1-265}$ to regulate $Ca_V1.2/Ca_V\beta1b$ channel current expression. Consistent with previous studies (16), tsA201 cells transiently co-transfected with GFP-tagged $Rem^{WT}$, $Ca_V1.2$, and $Ca_V\beta1b$ resulted in a complete loss of detectable ionic current expression (0.407 ± 0.392 pA/pF, n=8) (Fig. 4*C*, *D*). In contrast, currents measured from cells co-expressing channel components along with $Rem^{1-265}$ (−10.043 ± 2.837, n=14) were significantly different ($p < 0.01$) and displayed no inhibition of $Ca^{2+}$ channel activity (Fig. 4*C*, *D*). Taken together these data indicate that $Ca_V\beta$ subunit binding alone is not sufficient for Rem-mediated $Ca^{2+}$ channel blockade, and suggest that plasma membrane localization is a critical aspect of Rem-mediated channel regulation.

## The Isolated Rem C-terminus Does Not Regulate Channel Function

To determine whether the isolated Rem C-terminus was sufficient for $Ca^{2+}$ channel regulation, tsA201 cells were co-transfected with $Ca_V1.2$, $Ca_V\beta2a$, and either empty RFP or RFP-$Rem^{266-297}$ and currents were determined using the whole-cell configuration of the patch-clamp technique. Co-expression of RFP-$Rem^{266-297}$ (−17.712 ± 5.069, n=7) resulted in current not significantly different from that seen for channel components co-expressed with RFP (−22.275 ± 11.036, n=6) (Fig. 5*A*, current at 5 mV displayed in Fig. 5*B*), indicating that the isolated Rem C-terminus cannot regulate channel function. Confocal microscopy revealed that in contrast to full-length $Rem^{WT}$, $Rem^{266-297}$ was found

predominantly in punctate nuclear structures (Fig. 5*C*), suggesting that in the absence of the Rem GTP-binding core, the C-terminus acts as a nuclear localization signal.

### Plasma Membrane Localization is Critical for Rem-mediated $Ca^{2+}$ Channel Inhibition

To explore whether Rem-dependent $Ca^{2+}$ channel regulation requires molecular contacts between the C-terminus and known binding partners, such as calmodulin and 14-3-3, as suggested by recent studies (12–14), two chimeric proteins were created in which the C-terminus of K-Ras4B and H-Ras were fused to $Rem^{1-265}$ (Figure 6*A*). The resulting proteins were designated $Rem^{1-265}$/KRas4B-CAAX and $Rem^{1-265}$/HRas-CAAX. The K-Ras4B C-terminus is a well-characterized membrane targeting domain that contains a C-terminal polybasic domain, a farnesylation motif, and displays both PI lipid and calmodulin binding, maintaining many of the functional properties of the Rem C-terminus (23–25). On the other hand, the H-Ras targeting domain lacks a polybasic domain and does not bind calmodulin (24,25). Confocal imaging of GFP-tagged versions of both $Rem^{1-265}$/KRas4B-CAAX and $Rem^{1-265}$/HRas-CAAX displayed prominent localization to the cell periphery in a manner consistent with plasma membrane localization (Fig. 6*B*) and both proteins were found to co-immunoprecipitate with β2a (data not shown).

We postulated that plasma membrane targeting is required for Rem function. GFP-$Rem^{1-265}$/HRas-CAAX resulted in a strong reduction in detectable ionic current (−0.333 ± 0.422, n=14) when co-expressed with $Ca_V1.2$+β1b in tsA201 cells (Fig. 6*C*). Although GFP-$Rem^{1-265}$/KRas4B-CAAX was also targeted to the plasma membrane, it was found to only partially inhibit $Ca_V1.2$+β1b channel current expression (−1.827 ± 0.703, n=13), reducing inward currents by 81.8% when compared with control GFP-$Rem^{1-265}$ transfected tsA201 cells (Fig. 6*C*). Currents at 5 mV from channel complexes containing β1b co-expressed with GFP-$Rem^{1-265}$/KRas4B-CAAX were significantly different from those measured in the presence of GFP-$Rem^{1-265}$ ($p < 0.01$) but not significantly different from those channels co-expressed with GFP-$Rem^{1-265}$/HRas-CAAX (Fig. 6*E*). The relative potency of channel blockade was reversed when the fusion proteins were co-expressed with $Ca_V1.2$+β2a; GFP-$Rem^{1-265}$/KRas4B-CAAX resulted in strong inhibition of channel function (−0.376 ± 0.298, n=7) when compared with control cells (−16.93 ± 3.759, n=8), while GFP-$Rem^{1-265}$/HRas-CAAX inhibited inward current by 83.9% (−2.650 ± 0.748, n=11), (Fig. 6*D*). Currents at 5 mV from channel complexes containing β2a co-expressed with $Rem^{1-265}$/HRas-CAAX were significantly different from complexes co-expressed with GFP ($p < 0.01$) and complexes co-expressed with GFP-$Rem^{1-265}$/KRas4B-CAAX ($p < 0.01$) (Fig. 6*F*). These data suggest that plasma membrane localization is necessary for effective channel regulation but that the C-terminus of Rem may serve as more than a trafficking domain, since two distinct prenyl-mediated targeting sequences cannot functionally replace the Rem C-terminus.

## Discussion

To better characterize the mechanisms by which RGK proteins are regulated, we used confocal fluorescence microscopy to examine the role of the Rem C-terminus in plasma membrane localization and found that residues 270-282 play a critical role in this process (Fig. 1). Recent work by Heo and colleagues designed to examine the plasma membrane targeting mechanisms for a variety of small GTPases, including Rad and Gem, found that Ras family C-terminal domains containing polybasic motifs allow for direct association with both $PI(4,5)P_2$ and $PI(3,4,5)P_3$ lipids (23). The notion that a polybasic membrane targeting motif was required for Rem trafficking agrees with our localization data, as the loss of polybasic motifs in $Rem^{1-265}$ and $Rem^{1-270}$ prevented plasma membrane localization (Fig. 1*A*, *C*, *D*), while loss of one polybasic cluster in $Rem^{1-276}$ led to a significant reduction in membrane localization (Fig. 1*A*, *C*, *D*, *E*). In further support of this model, Rem was found to selectively bind phosphoinositides ($PIP_2$ and $PIP_3$) in an overlay assay using PIP strips,

and truncation of the C-terminus before position 282 resulted in a dramatic reduction in phosphatidylinositol lipid binding (Fig. 2). Taken together, these data suggest that the polybasic domains within the Rem C-terminus provide plasma membrane targeting specificity by binding to negatively charged $PIP_2$ and $PIP_3$ lipids in the plasma membrane, and that modulation of the membrane concentrations of these lipids may provide a molecular mechanism for regulating Rem signaling. Interestingly, previous studies have demonstrated potent upregulation of N- and L-type $Ca^{2+}$ channel function by $PI(3,4,5)P_3$ lipids (26), and that PI3K activation increases L-type $Ca^{2+}$ channel trafficking to the plasma membrane in a $Ca_V\beta2$-dependent fashion (27). It is possible, then, that the PI-mediated membrane association observed for Rem could serve as part of a negative feedback mechanism opposing an upregulation of channel function following an increase in $PI(3,4,5)P_3$ lipid concentration. Studies are ongoing to examine whether regulation of these lipid second messengers provides a novel mechanism for controlling Rem-dependent $Ca^{2+}$ channel inhibition.

Since Rem directly binds to a variety of accessory $Ca_V\beta$ subunits (9), and a number of studies suggest that this interaction is required for the regulation of functional $Ca^{2+}$ channels at the plasma membrane (8,9,11,16), we examined whether Rem localization would be altered by co-expression of either $Ca_V1.2$ or $Ca_V\beta$ subunits or in the presence of a functional $Ca_V1.2/\beta2a$ $Ca^{2+}$ channel. However, a similar fluorescence pattern was seen whether $Ca_V\alpha$ and/or $Ca_V\beta$ subunits were present or absent in tsA201 cells (Fig. 1*B*), indicating that plasma membrane trafficking of Rem is not dependent on $Ca^{2+}$ channel subunit expression. Beguin and colleagues report that wild-type RGK proteins display cytoplasmic, plasma membrane, and prominent nuclear localization when overexpressed in COS cells (12–14), a cellular distribution which is clearly different from that seen for GFP-Rem in tsA201 cells (Fig. 1). Whether these differences are cell line-specific or dependent on the level of Rem expression is unclear. Mutations within the C-terminus of RGK proteins that disrupt calmodulin binding have also been reported to promote nuclear translocation (12–14). Our data shows that $Rem^{1\text{-}265}$, $Rem^{1\text{-}270}$, and $Rem^{1\text{-}276}$ fail to bind calmodulin resin (Fig. 3*B*) and are not trafficked to the nucleus (Fig. 1*C*). However, the isolated Rem C-terminus expressed as an RFP fusion protein is localized to punctate structures within the nucleus, suggesting that the Rem C-terminus contains a cryptic nuclear localization sequence (Fig. 5*C*). While both $Rem^{WT}$ and $Rem^{1\text{-}282}$ displayed robust $Ca^{2+}$-dependent calmodulin binding and potent $Ca^{2+}$ channel blockade (Fig. 3), $Rem^{1\text{-}276}$ was shown to partially inhibit $Ca^{2+}$ channel function, yet this mutant is incapable of binding calmodulin resin (Fig. 3*B*). While these data indicate that calmodulin binding is not required for Rem-mediated $Ca^{2+}$ channel regulation, it might more subtly modulate Rem activity. Thus, it will be important in future studies to evaluate the effect of calmodulin and 14-3-3 binding, or site-selective phosphorylation within the polybasic domain, to modulate RGK protein plasma membrane targeting.

Previous studies have suggested an important role for the RGK C-terminus in both β-subunit binding and regulation of HVA channels (9,15,19), supporting the notion that β-subunit association was sufficient for RGK-mediated channel blockade. In this regard, the finding that truncation of the Rem C-terminus before residue 276 resulted in a reduced ability to associate with $Ca_V\beta2a$ when assayed by co-immunoprecipitation (Fig. 3*A*) was expected. However, the finding that $Rem^{1\text{-}276}$ associates with $Ca_V\beta2a$ just as well as $Rem^{WT}$, but does not completely block L-type $Ca^{2+}$ channel current expression in the presence of 30 mM $Ba^{2+}$ was unexpected (Fig. 3*C*). Furthermore, while $Rem^{1\text{-}270}$ had a reduced ability to co-immunoprecipitate $Ca_V\beta2a$, it was found to have no ability to inhibit $Ca^{2+}$ channel activity (Fig. 3*C*, *E*), suggesting that a β-binding threshold may exist for Rem-mediated $Ca^{2+}$ channel regulation, consistent with a recent report demonstrating dose-dependent RGK-mediated channel modulation (17). Because the loss of $Ca_V\beta2a$ binding seen with

progressive C-terminal deletions was mirrored by a reduction in plasma membrane trafficking (Figs. 3*A* and 1*D*), we examined whether this effect was specific for the palmitoylated $Ca_V\beta2a$ or whether $Rem^{1\text{-}265}$ would demonstrate a reduction in binding to another membrane-localized $Ca_V\beta$ subunit. In Figure 4*B* we find that $Rem^{1\text{-}265}$ binds the membrane-localized $Ca_V\beta$ isoform, $Ca_V\beta1b$, just as well as $Rem^{WT}$, suggesting that the loss of binding is specific for $Ca_V\beta2a$ and is not a consequence of reduced membrane localization for the Rem mutant. This notion is supported by *in vitro* pulldown assays which remove the complication of membrane localization from β-subunit interaction and demonstrate robust binding of $Rem^{1\text{-}265}$ to $Ca_V\beta2a$ (Fig. 4*A*). It is possible that the orientation in which the β subunit is anchored to the membrane affects the ability of Rem to bind, as it is known that β2a associates with the membrane through palmitoylation of its N-terminus, while the C-terminus of β1b is required for membrane association (3). Importantly, while the $Ca_V1.2/\beta1b$ channel is inhibited by wild-type Rem (Fig. 4*C*, *D*) (16), $Rem^{1\text{-}265}$ was unable to inhibit ionic current expression (Fig. 4*C*). There are two major conclusions that can be drawn from these studies. First, as deletion of the majority of the C-terminus does not disrupt $Ca_V\beta1b$ association *in vivo* or $Ca_V\beta2a$ *in vitro*, the β interaction domain is not located within the Rem C-terminus. Instead it appears to be located within the GTP-binding core of Rem and other RGK proteins (15,28). Secondly, since $Rem^{1\text{-}265}$ interacts with β1b but cannot regulate channel function (Fig. 4), $Ca_V\beta$ binding alone is not sufficient for Rem-mediated $Ca^{2+}$ channel regulation.

The observation that $Ca_V\beta$ subunit binding, unlike plasma membrane association, is not dependent upon the Rem C-terminus suggests that β binding and membrane localization are separable molecular events and each may serve as an independent means of regulating Rem activity. To isolate the role of membrane trafficking from other functions of the C-terminus, including PI lipid association (Fig. 2) and calmodulin binding (Fig. 3*B*) (14), we generated two chimeric $Rem^{1\text{-}265}$ variants (Fig. 6) using the membrane targeting domains from K-Ras4B and H-Ras (25). While the H-Ras CAAX domain relies upon prenylation/palmitoylation to direct membrane localization (25), the K-Ras4B region has many properties in common with Rem, including both calmodulin association and a polybasic domain capable of PI lipid-mediated PM targeting (23–25). Importantly, both anchors reconstituted plasma membrane association and partially restored $Ca^{2+}$ channel regulation (Fig. 6), in agreement with recent studies examining Rem2 function using a similar strategy (15). Therefore, directing plasma membrane association appears to be the primary function of the Rem C-terminus. However, since the chimeric proteins display more pronounced membrane trafficking (Fig. 6*B*) but do not fully recapitulate Rem-mediated $Ca^{2+}$ channel inhibition (Fig. 6*C*–*F*), it is likely that previously described interacting partners of and/or modifications to the Rem C-terminus (including PI lipids, calmodulin, and/or 14-3-3 association, or PKA/PKC-mediated phosphorylation), while not essential for channel regulation, may contribute to Rem signaling (12–14,18,20,23,29–33).

In summary, we have found that the Rem C-terminus serves as an essential targeting signal, likely acting through binding of the positively-charged polybasic region to negatively charged $PIP_2$ and $PIP_3$ lipids, to direct Rem plasma membrane association. While membrane localization and $Ca_V\beta$-subunit association are independent molecular events, we present strong evidence that both interactions play essential roles in Rem-mediated $Ca^{2+}$ channel regulation. This new function for the conserved RGK C-terminal domain provides an opportunity for a variety of physiological pathways to influence RGK signaling. Clearly, additional studies will be needed to clarify the role of phosphatidylinositol lipid signaling and calmodulin/14-3-3 binding in both Rem trafficking and $Ca^{2+}$ channel regulation.

## Acknowledgments

We wish to thank Dr. Carole L. Moncman for her expert assistance with the confocal imaging studies, Dr. Thomas C. Vanaman for the kind gift of calmodulin-sepharose resin, and members of the Andres lab for critical reading of this manuscript.

## The abbreviations used are

| | |
|---|---|
| **AID** | α-interaction domain |
| **RGK proteins** | Rem, Rem2, Rad, and Gem/Kir GTPases |
| **GST** | glutathione *S*-transferase |
| **HEK** | human embryonic kidney |
| **GFP** | green fluorescent protein |
| **HA** | hemagglutinin |
| **GTPγS** | guanosine 5′-3-*O*-(thio)triphosphate or guanosine 5′-*O*-(thiotriphosphate) |
| **WT** | wild type |
| **pA** | picoampere |
| **pF** | picofarad |
| **BSA** | bovine serum albumin |
| **PI** | phosphatidylinositol |

## References

1. Catterall WA. Structure and regulation of voltage-gated Ca2+ channels. Annu Rev Cell Dev Biol. 2000; 16:521–55. [PubMed: 11031246]
2. Richards MW, Butcher AJ, Dolphin AC. Ca2+ channel beta-subunits: structural insights AID our understanding. Trends Pharmacol Sci. 2004; 25:626–32. [PubMed: 15530640]
3. Dolphin AC. Beta subunits of voltage-gated calcium channels. J Bioenerg Biomembr. 2003; 35:599–620. [PubMed: 15000522]
4. Finlin BS, Andres DA. Rem is a new member of the Rad- and Gem/Kir Ras-related GTP-binding protein family repressed by lipopolysaccharide stimulation. J Biol Chem. 1997; 272:21982–8. [PubMed: 9268335]
5. Finlin BS, Shao H, Kadono-Okuda K, Guo N, Andres DA. Rem2, a new member of the Rem/Rad/Gem/Kir family of Ras-related GTPases. Biochem J. 2000; 347(Pt 1):223–31. [PubMed: 10727423]
6. Reynet C, Kahn CR. Rad: a member of the Ras family overexpressed in muscle of type II diabetic humans. Science. 1993; 262:1441–4. [PubMed: 8248782]
7. Maguire J, Santoro T, Jensen P, Siebenlist U, Yewdell J, Kelly K. Gem: an induced, immediate early protein belonging to the Ras family. Science. 1994; 265:241–4. [PubMed: 7912851]
8. Beguin P, Nagashima K, Gonoi T, Shibasaki T, Takahashi K, Kashima Y, Ozaki N, Geering K, Iwanaga T, Seino S. Regulation of Ca2+ channel expression at the cell surface by the small G-protein kir/Gem. Nature. 2001; 411:701–6. [PubMed: 11395774]
9. Finlin BS, Crump SM, Satin J, Andres DA. Regulation of voltage-gated calcium channel activity by the Rem and Rad GTPases. Proc Natl Acad Sci U S A. 2003; 100:14469–74. [PubMed: 14623965]
10. Finlin BS, Mosley AL, Crump SM, Correll RN, Ozcan S, Satin J, Andres DA. Regulation of L-type Ca2+ channel activity and insulin secretion by the Rem2 GTPase. J Biol Chem. 2005; 280:41864–71. [PubMed: 15728182]
11. Sasaki T, Shibasaki T, Beguin P, Nagashima K, Miyazaki M, Seino S. Direct inhibition of the interaction between alpha-interaction domain and beta-interaction domain of voltage-dependent Ca2+ channels by Gem. J Biol Chem. 2005; 280:9308–12. [PubMed: 15615719]

12. Beguin P, Mahalakshmi RN, Nagashima K, Cher DH, Takahashi A, Yamada Y, Seino Y, Hunziker W. 14-3-3 and calmodulin control subcellular distribution of Kir/Gem and its regulation of cell shape and calcium channel activity. J Cell Sci. 2005; 118:1923–34. [PubMed: 15860732]
13. Beguin P, Mahalakshmi RN, Nagashima K, Cher DH, Kuwamura N, Yamada Y, Seino Y, Hunziker W. Roles of 14-3-3 and calmodulin binding in subcellular localization and function of the small G-protein Rem2. Biochem J. 2005; 390:6775.
14. Beguin P, Mahalakshmi RN, Nagashima K, Cher DH, Ikeda H, Yamada Y, Seino Y, Hunziker W. Nuclear sequestration of beta-subunits by Rad and Rem is controlled by 14-3-3 and calmodulin and reveals a novel mechanism for Ca2+ channel regulation. J Mol Biol. 2006; 355:34–46. [PubMed: 16298391]
15. Chen H, Puhl HL 3rd, Niu SL, Mitchell DC, Ikeda SR. Expression of Rem2, an RGK family small GTPase, reduces N-type calcium current without affecting channel surface density. J Neurosci. 2005; 25:9762–72. [PubMed: 16237180]
16. Finlin BS, Correll RN, Pang C, Crump SM, Satin J, Andres DA. Analysis of the complex between Ca2+ channel beta-subunit and the Rem GTPase. J Biol Chem. 2006; 281:23557–66. [PubMed: 16790445]
17. Seu L, Pitt GS. Dose-dependent and isoform-specific modulation of Ca2+ channels by RGK GTPases. J Gen Physiol. 2006; 128:605–13. [PubMed: 17074979]
18. Crump SM, Correll RN, Schroder EA, Lester WC, Finlin BS, Andres DA, Satin J. L-type calcium channel alpha-subunit and protein kinase inhibitors modulate Rem-mediated regulation of current. Am J Physiol Heart Circ Physiol. 2006; 291:H1959–71. [PubMed: 16648185]
19. Kelly K. The RGK family: a regulatory tail of small GTP-binding proteins. Trends Cell Biol. 2005; 15:640–3. [PubMed: 16242932]
20. Ward Y, Spinelli B, Quon MJ, Chen H, Ikeda SR, Kelly K. Phosphorylation of critical serine residues in Gem separates cytoskeletal reorganization from down-regulation of calcium channel activity. Mol Cell Biol. 2004; 24:651–61. [PubMed: 14701738]
21. Andres DA, Crump SM, Correll RN, Satin J, Finlin BS. Analyses of Rem/RGK Signaling and Biological Activity. Methods Enzymol. 2005; 407:484–98. [PubMed: 16757347]
22. Pan JY, Fieles WE, White AM, Egerton MM, Silberstein DS. Ges, A human GTPase of the Rad/Gem/Kir family, promotes endothelial cell sprouting and cytoskeleton reorganization. J Cell Biol. 2000; 149:1107–16. [PubMed: 10831614]
23. Heo WD, Inoue T, Park WS, Kim ML, Park BO, Wandless TJ, Meyer T. PI(3,4,5)P3 and PI(4,5)P2 lipids target proteins with polybasic clusters to the plasma membrane. Science. 2006; 314:1458–61. [PubMed: 17095657]
24. Villalonga P, Lopez-Alcala C, Bosch M, Chiloeches A, Rocamora N, Gil J, Marais R, Marshall CJ, Bachs O, Agell N. Calmodulin binds to K-Ras, but not to H- or N-Ras, and modulates its downstream signaling. Mol Cell Biol. 2001; 21:7345–54. [PubMed: 11585916]
25. Plowman SJ, Hancock JF. Ras signaling from plasma membrane and endomembrane microdomains. Biochim Biophys Acta. 2005; 1746:274–83. [PubMed: 16039730]
26. Blair LA, Marshall J. IGF-1 modulates N and L calcium channels in a PI 3-kinase-dependent manner. Neuron. 1997; 19:421–9. [PubMed: 9292730]
27. Viard P, Butcher AJ, Halet G, Davies A, Nurnberg B, Heblich F, Dolphin AC. PI3K promotes voltage-dependent calcium channel trafficking to the plasma membrane. Nat Neurosci. 2004; 7:939–46. [PubMed: 15311280]
28. Opatowsky Y, Sasson Y, Shaked I, Ward Y, Chomsky-Hecht O, Litvak Y, Selinger Z, Kelly K, Hirsch JA. Structure-function studies of the G-domain from human gem, a novel small G-protein. FEBS Lett. 2006; 580:5959–64. [PubMed: 17052716]
29. Fischer R, Wei Y, Anagli J, Berchtold MW. Calmodulin binds to and inhibits GTP binding of the ras-like GTPase Kir/Gem. J Biol Chem. 1996; 271:25067–70. [PubMed: 8810259]
30. Zhu J, Reynet C, Caldwell JS, Kahn CR. Characterization of Rad, a new member of Ras/GTPase superfamily, and its regulation by a unique GTPase-activating protein (GAP)-like activity. J Biol Chem. 1995; 270:4805–12. [PubMed: 7876254]
31. Moyers JS, Bilan PJ, Zhu J, Kahn CR. Rad and Rad-related GTPases interact with calmodulin and calmodulin-dependent protein kinase II. J Biol Chem. 1997; 272:11832–9. [PubMed: 9115241]

32. Moyers JS, Zhu J, Kahn CR. Effects of phosphorylation on function of the Rad GTPase. Biochem J. 1998; 333 ( Pt 3):609–14. [PubMed: 9677319]

33. Finlin BS, Andres DA. Phosphorylation-dependent association of the Ras-related GTP-binding protein Rem with 14-3-3 proteins. Arch Biochem Biophys. 1999; 368:401–12. [PubMed: 10441394]

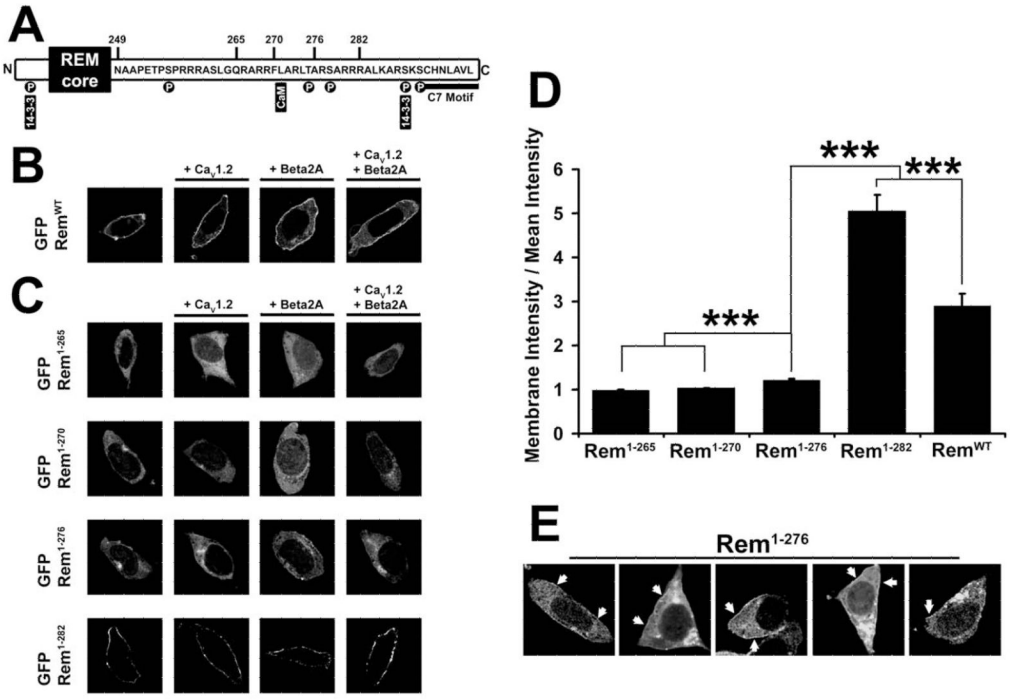


**Figure 1. Deletion of the Rem C-terminus prevents plasma membrane localization**

(A) Diagram showing features of the Rem C-terminus and the locations of Rem truncations. (B) TsA201 cells were transfected with plasmids expressing Rem$^{WT}$ and either empty pCMVT7F2 vector, Ca$_V$1.2 and/or Flag-Ca$_V$β2a. 72 hours post-transfection, cells were examined by confocal microscopy. The localization of Rem$^{WT}$ at the cell periphery is not significantly affected by co-expression of calcium channel components. (C) TsA201 cells were transfected with plasmids expressing Rem truncations and either empty pCMVT7F2 vector, Ca$_V$1.2 and/or Flag-Ca$_V$β2a, as described in Figure 1B. GFP-Rem$^{1-265}$ and GFP-Rem$^{1-270}$ show cytosolic localization, GFP-Rem$^{1-276}$ shows slight cell periphery enrichment, and GFP-Rem$^{1-282}$ displays very strong cell periphery enrichment consistent with plasma membrane localization irrespective of Ca$_V$β2a or Ca$_V$1.2 co-transfection. (D) Confocal images were quantified by line-scan from the cytosolic interior of the cell to the plasma membrane as described under “Experimental Procedures”. Intensity at the cell periphery was divided by the mean intensity over the total line-scan to find cell peripheral enrichment. Line-scan was performed four times for each cell examined and the results averaged. A significant difference ($p<0.05$) between treatments is denoted by asterisks. (E) Selection of tsA201 cells from Figures 1C and 1D. Arrows indicate patches of increased GFP-Rem$^{1-276}$ expression at the cell boundary.

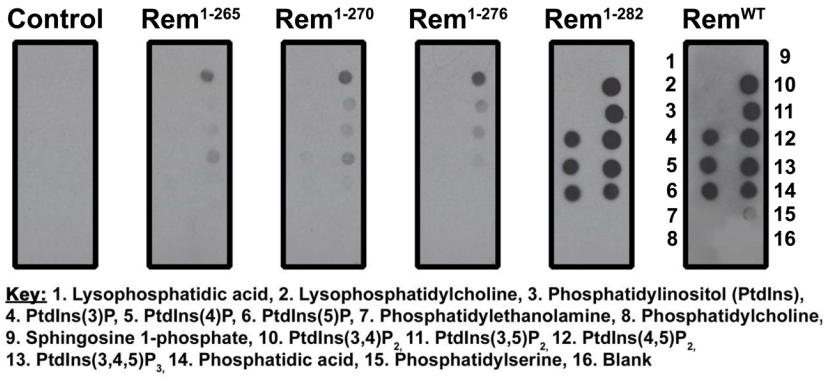


**Figure 2. Rem membrane localization is positively correlated to PI lipid association**

3xFlag-tagged Rem truncations or empty 3xFlag vector (control) were overexpressed in tsA201 cells and cell lysates were exposed to PIP strips in an overlay assay. Association of Rem truncations with spotted lipids was observed using immunoblotting with biotinylated FLAG antibody. Although $Rem^{1-282}$ and $Rem^{WT}$ display robust association with phosphorylated PI lipids, further truncation of the Rem C-terminus dramatically diminishes the interaction.

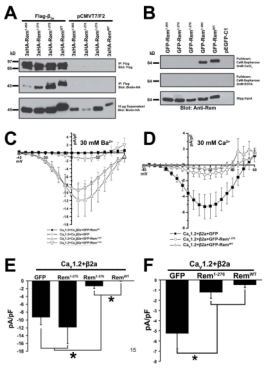


**Figure 3. β2a association is not sufficient for Rem-mediated $Ca^{2+}$ channel regulation**

(A) HEK293 cells were transfected with 3xHA-Rem truncations and either empty pCMVT7F2 (FLAG) vector or Flag-$Ca_V$β2a. Co-immunoprecipitation was performed with Flag antibody and interaction with Rem examined by immunoblotting with biotinylated anti-HA antibody. (B) TsA201 cells were transfected with plasmids expressing GFP-$Rem^{1-265}$, GFP-$Rem^{1-270}$, GFP-$Rem^{1-276}$, GFP-$Rem^{1-282}$, GFP-$Rem^{WT}$, or empty pEGFP-C1 as control. Lysates were pulled down onto calmodulin-sepharose beads in the presence of 2 mM $CaCl_2$ or 2.5 mM EGTA, beads were boiled to release bound protein, and the ability of Rem truncations to associate with calmodulin was examined by immunoblotting with anti-Rem antibody. (C) HEK293 cells were transfected with plasmids expressing $Ca_V1.2$, Flag-$Ca_V$β2a, and either GFP-$Rem^{1-270}$, GFP-$Rem^{1-276}$, GFP-$Rem^{WT}$ or empty pEGFP-C1 as control. Current through $Ca_V1.2$+$Ca_V$β2a complex was examined using the whole-cell patch clamp configuration in the presence of 30 mM $Ba^{2+}$. (D) TsA201 cells were transfected with plasmids expressing $Ca_V1.2$, Flag-$Ca_V$β2a, and either GFP-$Rem^{1-276}$, GFP-$Rem^{WT}$ or empty pEGFP-C1 as control. Current through $Ca_V1.2$+$Ca_V$β2a complex was examined using the whole-cell patch clamp configuration in the presence of 30 mM $Ca^{2+}$. (E) Currents at 5 mV from Figure 3*C*. A significant difference ($p<0.05$) between treatments is denoted by asterisks. (F) Currents at 5 mV from Figure 3*D*. A significant difference ($p<0.05$) between treatments is denoted by asterisks.

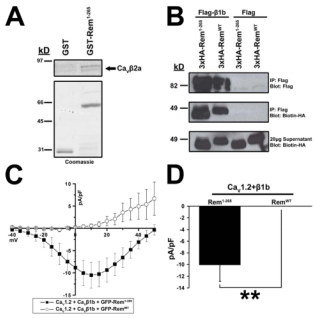


**Figure 4. Rem$^{1-265}$ can bind Ca$_V$β1b but cannot regulate channel function**

(A) GST or GST-tagged Rem$^{1-265}$ protein was incubated with $^{35}$S labeled Ca$_V$β2a in the presence of glutathione sepharose. Bound proteins were eluted by addition of free glutathione, resolved via SDS-PAGE, and Ca$_V$β2a association observed via autoradiography. (B) TsA201 cells were transfected with plasmids expressing Rem$^{WT}$, Rem$^{1-265}$ and either empty pCMVT7F2 vector control or Flag-Ca$_V$β1b. Co-immunoprecipitation was performed with Flag antibody and interaction with Rem proteins examined by immunoblotting with biotinylated HA antibody. Rem$^{1-265}$ and Rem$^{WT}$ were both capable of binding Ca$_V$β1b. (C) TsA201 cells were transfected with plasmids expressing Ca$_V$1.2, Flag-Ca$_V$β1b, and either GFP-Rem$^{1-265}$ or empty pEGFP-C1 as control. Current through Ca$_V$1.2+Ca$_V$β1b complex examined using the whole-cell patch clamp configuration. (D) Currents at 5 mV from Figure 4C. A significant difference ($p<0.05$) between treatments is denoted by asterisks.

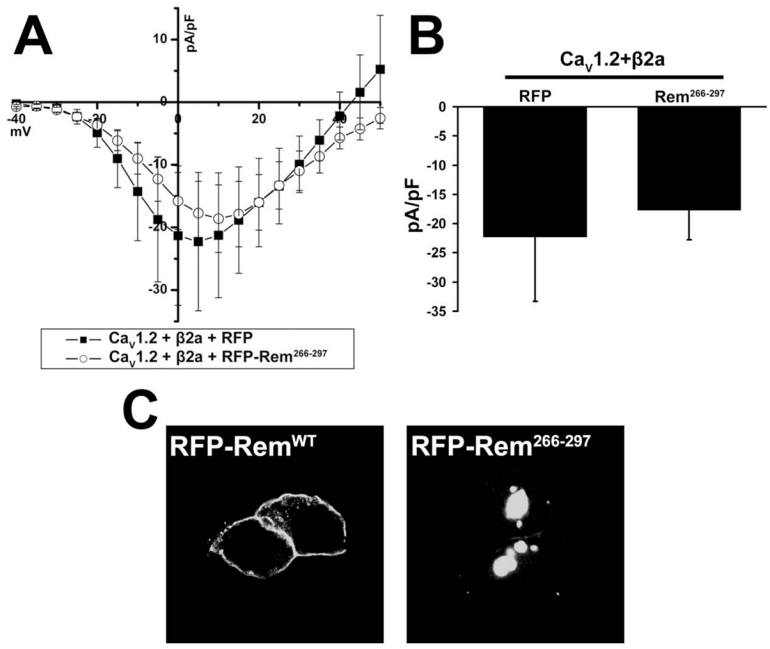


**Figure 5. The isolated Rem C-terminus does not inhibit $Ca^{2+}$ channel current**

(A) TsA201 cells were co-transfected with $Ca_V1.2$, β2a, and either RFP or RFP-$Rem^{266-297}$, and current was examined using the whole-cell patch clamp configuration. (B) Currents at 5 mV from Figure 5A. There is no significant difference between the treatments. (C) TsA201 cells expressing either RFP-$Rem^{WT}$ or RFP-$Rem^{266-297}$ were analyzed 72 h after post-transfection, by confocal microscopy.

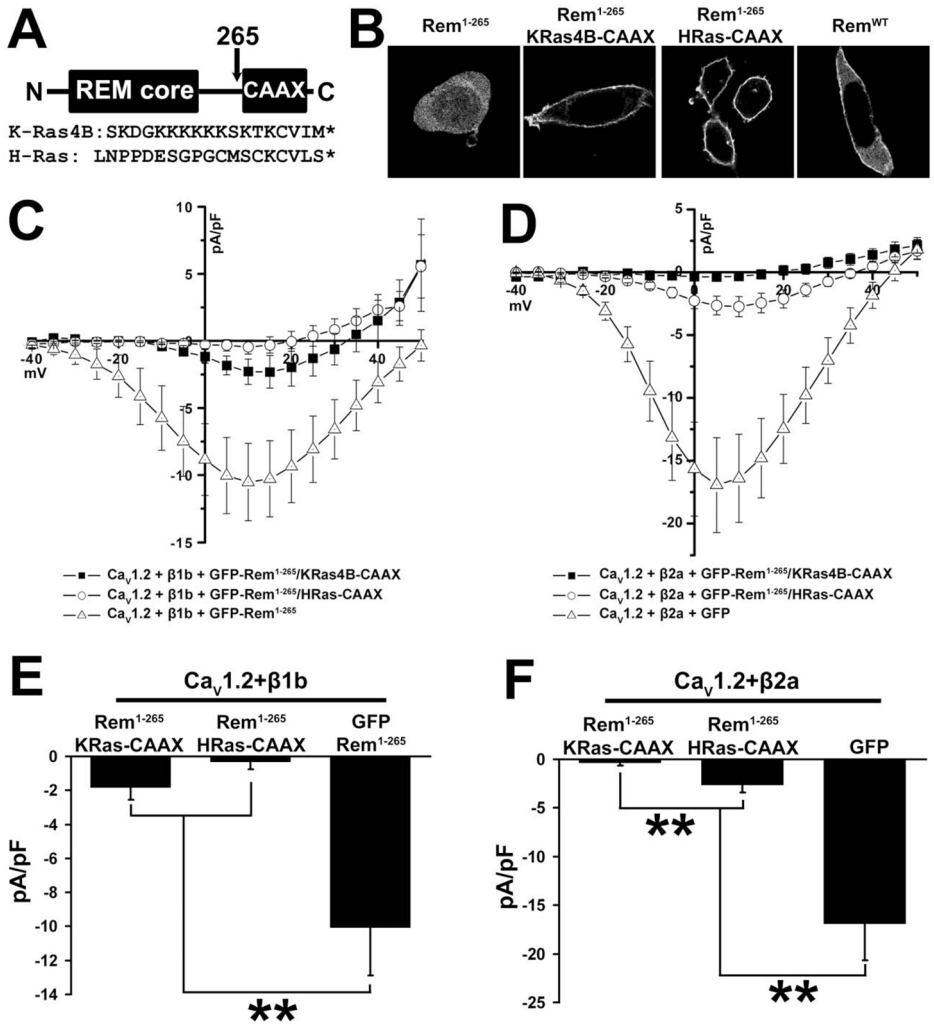


**Figure 6. Membrane-targeted Rem$^{1-265}$ inhibits $I_{Ca}$**

(A) Diagram showing construction of CAAX chimeric proteins and sequences of the K-Ras4B and H-Ras C-terminal and CAAX domains. (B) TsA201 cells were transfected with plasmids expressing GFP-Rem$^{1-265}$, GFP-Rem$^{1-265}$/KRas4B-CAAX, GFP-Rem$^{1-265}$/HRas-CAAX, or GFP-Rem$^{WT}$. 72 h after transfection cells were observed by confocal microscopy. Rem$^{1-265}$ shows cytosolic localization, but fusion of either of the CAAX tags results in cell peripheral distribution stronger even than that of Rem$^{WT}$ and consistent with plasma membrane localization. (C) TsA201 cells were transfected with plasmids expressing $Ca_V1.2$, $Ca_V\beta1b$, and either GFP-Rem$^{1-265}$, GFP-Rem$^{1-265}$/KRas4B-CAAX, or GFP-Rem$^{1-265}$/HRas-CAAX. Although GFP-Rem$^{1-265}$/HRas-CAAX can fully inhibit the activity of this channel complex, GFP-Rem$^{1-265}$/KRas4B-CAAX shows only partial inhibition. (D) TsA201 cells were transfected with plasmids expressing $Ca_V1.2$, $Ca_V\beta2a$, and either GFP-Rem$^{1-265}$/KRas4B-CAAX, GFP-Rem$^{1-265}$/HRas-CAAX, or GFP as a control. Although GFP-Rem$^{1-265}$/KRas4B-CAAX can fully inhibit the activity of this channel complex, GFP-Rem$^{1-265}$/HRas-CAAX shows only partial inhibition. (E) Currents at 5 mV from Figure 6C. A significant difference ($p<0.05$) between treatments is denoted by asterisks. (F) Currents at 5 mV from Figure 6D. A significant difference ($p<0.05$) between treatments is denoted by asterisks.

## Table I

### Electrophysiological Parameters of Analyzed Currents†

The values Gmax, $V_{1/2}$, Erev and k are reported for all patch-clamp recordings. Values were derived as described in "Experimental Procedures".

| Figure 3C | Solution (mM) | Gmax (μS/pF) | ±SE | n* | $V_{1/2}$ (mV) | ±SE | Erev (mV) | ±SE | k | ±SE | n |
|---|---|---|---|---|---|---|---|---|---|---|---|
| $Ca_V1.2$+Flag-β2a+GFP | 30 $Ba^{2+}$ | 0.2885 | ±0.05983 | 7 | −7.8 | ±1.5 | 41.3 | ±1.9 | 6.3 | ±0.3 | 7 |
| $Ca_V1.2$+Flag-β2a+GFP-$Rem^{1-270}$ | 30 $Ba^{2+}$ | 0.4868 | ±0.1489 | 8 | −2.2 | ±1.2 | 42.9 | ±3.2 | 6.8 | ±0.3 | 8 |
| $Ca_V1.2$+Flag-β2a+GFP-$Rem^{1-276}$ | 30 $Ba^{2+}$ | 0.1433 | ±0.03796 | 7 | 3.9 | ±1.6 | 46.3 | ±7.3 | 7.4 | ±0.7 | 5 |
| $Ca_V1.2$+Flag-β2a+GFP-$Rem^{WT}$ | 30 $Ba^{2+}$ | 0.01517 | ±0.01592 | 4 | NA | NA | NA | NA | NA | NA | 0 |
| Figure 3D | | | | | | | | | | | |
| $Ca_V1.2$+Flag-β2a+GFP | 30 $Ca^{2+}$ | 0.1735 | ±0.04717 | 11 | 3.8 | ±1.4 | 63.8 | ±5.1 | 8.4 | ±0.3 | 7 |
| $Ca_V1.2$+Flag-β2a+GFP-$Rem^{1-276}$ | 30 $Ca^{2+}$ | NA‡ | NA‡ | | NA‡ | NA‡ | NA‡ | NA‡ | NA‡ | NA‡ | |
| $Ca_V1.2$+Flag-β2a+GFP-$Rem^{WT}$ | 30 $Ca^{2+}$ | NA‡ | NA‡ | | NA‡ | NA‡ | NA‡ | NA‡ | NA‡ | NA‡ | |
| Figure 4C | | | | | | | | | | | |
| $Ca_V1.2$+Flag-β1b+GFP-$Rem^{1-265}$ | 30 $Ba^{2+}$ | 0.3872 | ±0.08978 | 14 | 0.8 | ±3.0 | 44.1 | ±3.8 | 7 | ±0.3 | 11 |
| $Ca_V1.2$+Flag-β1b+GFP-$Rem^{WT}$ | 30 $Ba^{2+}$ | 0.1897 | ±0.1055 | 8 | NA | NA | NA | NA | NA | NA | 0 |
| Figure 5A | | | | | | | | | | | |
| $Ca_V1.2$+Flag-β2a+RFP | 30 $Ba^{2+}$ | 0.6893 | ±0.3782 | 6 | −5.2 | ±1.1 | 43.5 | ±6.6 | 6.7 | ±0.5 | 5 |
| $Ca_V1.2$+Flag-β2a+RFP-$Rem^{266-296}$ | 30 $Ba^{2+}$ | 0.5959 | ±0.1897 | 7 | −1.1 | ±1.9 | 52.2 | ±4.2 | 8.171 | ±0.5 | 7 |
| Figure 6C | | | | | | | | | | | |
| $Ca_V1.2$+Flag-β1b+GFP-$Rem^{1-265}$/KRasCAAX | 30 $Ba^{2+}$ | 0.2375 | ±0.09177 | 13 | 9 | ±1.8 | 43.9 | ±3.2 | 6.5 | ±0.4 | 7 |
| $Ca_V1.2$+Flag-β1b+GFP-$Rem^{1-265}$/HRasCAAX | 30 $Ba^{2+}$ | 0.2075 | ±0.09102 | 14 | 5.9 | ±1.8 | 53.7 | ±6.2 | 6.8 | ±0.3 | 3 |
| $Ca_V1.2$+Flag-β1b+GFP-$Rem^{1-265}$ | 30 $Ba^{2+}$ | 0.3872 | ±0.08978 | 14 | 0.8 | ±3.0 | 44.1 | ±3.8 | 7 | ±0.3 | 11 |
| Figure 6D | | | | | | | | | | | |
| $Ca_V1.2$+Flag-β2a+GFP-$Rem^{1-265}$/KRasCAAX | 30 $Ba^{2+}$ | 0.06601 | ±0.01510 | 7 | −2.8 | ±0.1 | 52.1 | ±11.1 | 6.2 | ±1.0 | 2 |
| $Ca_V1.2$+Flag-β2a+GFP-$Rem^{1-265}$/HRasCAAX | 30 $Ba^{2+}$ | 0.1357 | ±0.03902 | 11 | 0.6 | ±1.5 | 41.3 | ±3.3 | 6.9 | ±0.5 | 8 |
| $Ca_V1.2$+Flag-β2a+GFP | 30 $Ba^{2+}$ | 0.5013 | ±0.06228 | 28 | −3.8 | ±1.0 | 42.6 | ±1.6 | 6.8 | ±0.3 | 26 |

† Boltzmann form used: $I(V)=Gmax*(V-Erev)/(1+\exp(V_{1/2}-V)/k)$

* Measurements taken only from cells with detectable current except for Gmax, which was taken from all cells, with and without current.

‡Boltzmann fit failed for this dataset -- current amplitude was too small to define an inflection point on the ascending limb of the activation curve.